Polymer Melt Intercalation in Organically-Modified Layered Silicates: Model Predictions and Experiment

Richard A. Vaia*,† and Emmanuel P. Giannelis*

Department of Materials Science and Engineering, Cornell University, Ithaca, New York 14853

Received March 5, 1996; Revised Manuscript Received September 16, 1997[⊗]

ABSTRACT: The effect of silicate functionalization, anneal temperature, polymer molecular weight, and constituent interactions on polymer melt intercalation of a variety of styrene-derivative polymers in alkylammonium-functionalized silicates is examined. Hybrid formation requires an optimal interlayer structure for the organically-modified layered silicate (OLS), with respect to the number per host area and size of the alkylammonium chains, as well as the presence of polar interactions between the OLS and polymer. From these observations and the qualitative predictions of the mean-field lattice-based model of polymer melt intercalation (preceding paper in this issue), general guidelines may be established for selecting potentially compatible polymer−OLS systems. The interlayer structure of the OLS should be optimized to maximize the configurational freedom of the functionalizing chains upon layer separation while maximizing potential interaction sites with the surface. The most successful polymers for intercalation exhibited polar character or contained Lewis-acid/base groups.

1. Introduction

Polymer melt intercalation of mica-type layered silicates is a viable approach to synthesize a variety of polymer−silicate nanocomposites.[1−6] These hybrids exhibit improved modulus,[7−9] decreased thermal expansion coefficient,[8] reduced gas permeability,[8,10] increased solvent resistance,[6] and enhanced ionic conductivity[3,11] when compared to the pristine polymers. Furthermore, polymer-silicate nanocomposites, in addition to their potential applications, are unique model systems to study the structure and dynamics of polymers in confined environments.[4,5,12,13]

The nanoscale layered structure of the mica-type silicate leads to hybrids with nanoscale phase dimensions. Mica-type layered silicates, MTS's, (alternatively referred to as 2:1 layered silicates) possess the same structural characteristics as the well-known minerals talc and mica.[14−16] Their crystal structure consists of two-dimensional layers (thickness = 0.95 nm) formed by fusing two silica tetrahedral sheets with an edge-shared octahedral sheet of either alumina or magnesia. Stacking of the layers leads to van der Waals gaps or galleries. The galleries (alternatively referred to as interlayers) are occupied by cations which balance the charge deficiency that is generated by isomorphous substitution within the layers (e.g. Al for Si or Mg for Al). In contrast to pristine mica-type silicates which contain alkali metal and alkali earth charge-balancing cations, organically-modified layered silicates (OLS) contain alkylammonium or alkylphosphonium cations.[17,18] The presence of these organic-modifiers in the galleries renders the originally hydrophilic silicate surface organophilic. Depending on the functionality, packing density, and length of the organic modifiers, the OLS's may be engineered to optimize their compatibility with a given polymer.

Nanocomposite synthesis via polymer melt intercalation involves annealing, statically or under shear, a mixture of polymer and layered silicate above the softening point of the polymer. During the anneal, polymer chains diffuse from the bulk polymer melt into the interlayers or galleries between the silicate layers. Depending on the degree of penetration of the polymer into the MTS framework, hybrids are obtained with structures ranging from *intercalated* to *exfoliated*. Polymer penetration resulting in finite expansion of the silicate layers produces intercalated hybrids consisting of well-ordered multilayers with alternating polymer/silicate layers and a repeat distance of a few nanometers. Extensive polymer penetration resulting in delamination of the silicate layers produces exfoliated hybrids consisting of individual nanometer-thick silicate layers suspended in a polymer matrix. In contrast, if the polymer and the silicate are immiscible, macro- instead of nanocomposites are formed. These macroscale hybrids consist of agglomerates of the layered silicate (sometimes as large as 1 mm in diameter) surrounded by polymer and resemble conventional filled rubbers and plastics.

With organically-modified layered silicates, nanocomposites have been obtained from a large spectrum of polymers with varying degrees of polarity and chain rigidity, including polycarbonates, polymethacrylates, polysiloxanes, polyphosphazenes, and main-chain liquid-crystalline polymers.[19] Whether an admixture of polymer and OLS produces an exfoliated or intercalated nanocomposite or a conventional macrocomposite depends critically upon the characteristics of the polymer and the OLS. These characteristics include the nature of the polymer as well as the type, packing density, and size of the organic modifiers on the silicate surface. Unfortunately, existing guidelines as to the optimum polymer−OLS combination have proven unsatisfactory and, at times, contradictory. Consequently, hybrid synthesis is currently a tedious trial-and-error process.

In the preceding paper in this issue, we presented a mean-field, lattice-based description of polymer melt intercalation in organically-modified layered silicates.[1] In general, an interplay of entropic and energetic factors determines the outcome of polymer melt intercalation. Free energy plots and their dependence on internal energy and entropy suggest three possible equilibrium states—immiscible, intercalated, and exfoliated—all of which have been experimentally observed.

† Present address: Polymer Branch, Materials Directorate, Air Force Research Laboratory, Wright-Patterson AFB, OH 45433.

⊗ Abstract published in *Advance ACS Abstracts,* November 15, 1997.

S0024-9297(96)00348-8 CCC: $14.00

In the current paper, we report how various characteristics of the silicate and polymer, including silicate functionalization, anneal temperature, molecular weight of the polymer, and constituent interactions, affect hybrid formation. By comparing the experimental results with the theoretical predictions of the mean-field model, we then propose general guidelines governing hybrid formation.

2. Thermodynamic Model

The thermodynamic aspects of hybrid formation may be examined using the mean-field, lattice-based description of polymer melt intercalation as discussed previously.[1] A great advantage of the model is the ability to analytically determine the effect on hybrid formation of various characteristics of the polymer and OLS. Briefly, the free energy change per interlayer volume, Δf_V, associated with polymer intercalation, may be expressed as

$$\Delta f_V = \Delta e_V - T\Delta s_V \tag{1}$$

Δe_V and Δs_V are the internal energy and entropy change per interlayer volume, respectively, and

$$\Delta s_V = N_A k_B[\Delta s_V^{chain} + \Delta s_V^{polymer}]$$

$$= N_A k_B\left[\frac{\hat{\varphi}_2}{\nu_2}\ln(c)(\chi_S - \chi_{S0}) - \frac{\hat{\varphi}_1}{\nu_1}\left\{\frac{\pi^2}{6}\left(\frac{a_1}{h}\right)^2 + \sqrt{3}\frac{u}{\sqrt{m_1}}\frac{a_1}{h}\right\}\right] \tag{2}$$

$$\Delta e_V = \hat{\varphi}_1\hat{\varphi}_2\frac{1}{Q}\left(\frac{2}{h_0}\epsilon_{sp,sa} + \frac{2}{r_2}\epsilon_{ap}\right) \tag{3}$$

Δs_V is expressed as the sum of the entropy change associated with the organically-modified silicate, Δs_V^{chain}, and the entropy change associated with the confinement of the polymer, $\Delta s_V^{polymer}$. h_0 and h are the initial and after polymer intercalation gallery height, respectively. m_i, ν_i, $\hat{\varphi}_i$, r_i, and a_i are the number of segments per chain, the molar volume per segment, the interlayer volume fraction, the radius of the interaction surface, and the segment length of the ith interlayer species. u is a dimensionless excluded volume parameter, Q is a constant near unity, and χ_S and χ_{S0} are the fraction of interlayer volume near the surface at height h and h_0, respectively, which influence the potential chain conformations. ϵ_{ap} represents the pairwise interaction energy per area between the aliphatic chains and the polymer and $\epsilon_{sp,sa} = \epsilon_{sp} - \epsilon_{sa}$, is the difference between the pairwise interaction energy per area between the aliphatic chain and the surface, ϵ_{sa}, and that between the polymer and the surface, ϵ_{sp}. A detailed discussion of the model including the different variables may be found in the preceding paper.[1]

Values for the geometrical parameters can be found in the general literature for a variety of polymers.[20] In contrast, the as-defined values for the interaction parameters of an incompressible system are unavailable. However, since the model is mean-field, the microscopic pairwise interaction energies per area, ϵ_{jk} may be expressed as an interfacial energy between species j and k, γ_{jk}. Then, $\epsilon_{ap} \sim \gamma_{ap}$ and $\epsilon_{sp,sa} \sim \Delta\gamma_s$.

The polar and apolar components of the constituent interactions may be separately examined using expressions for interfacial tension such as those developed by van Oss and co-workers.[21−23] From their expressions,[21−23] the surface energy, γ_j, is comprised of an apolar component, (γ_j^{LW}, Lifschitz−van der Waals) and a polar/associative component (γ_j^{AB}, Lewis acid/base). The Lifschitz−van der Waals component arises from dispersive and dipolar interactions, whereas the polar component arises from associative-type interactions. For the polar component, two parameters must be specified, one describing the electron acceptor character, γ_j^+, and one describing the electron donor character, γ_j^-, with $\gamma_j^{AB} = 2(\gamma_j^+\gamma_j^-)^{1/2}$. Using the geometric combination rule, the total interfacial energy between species j and k is

$$\gamma_{jk} = \gamma_{jk}^{LW} + \gamma_{jk}^{AB} \tag{4}$$

where γ_{jk}^{LW} and γ_{jk}^{AB} are the polar and apolar components of the interactions, respectively, and

$$\gamma_{jk}^{LW} = (\sqrt{\gamma_j^{LW}} - \sqrt{\gamma_k^{LW}})^2 \tag{5}$$

$$\gamma_{jk}^{AB} = 2(\sqrt{\gamma_j^+} - \sqrt{\gamma_j^-} - \sqrt{\gamma_k^-}) \tag{6}$$

These expressions provide a means to approximate the relative magnitude and sign of the pair/wise interaction parameters using available experimental values. Most importantly, they can be used to identify the range of interactions that is most favorable for hybrid formation.

Table 1. Polymer Characteristics

	abbreviation	$\bar{M}_W$	$\bar{M}_W/\bar{M}_N$	T_g, °C
polystyrene	PS30	30 000	1.06	96
	PS90	90 000	1.06	100
	PS400	400 000	1.06	100
poly(3-bromostyrene)	PS3Br	55 000	2.00	113
poly(vinylcyclohexane)	PVCH	97 000		120
poly(2-vinylpyridine)	PVP	150 000	2.10	104

3. Experimental Methods

3.1. Materials and Synthesis. Organically-modified layered silicates were synthesized by a cation exchange reaction between the layered silicate host and excess alkylammonium cations, as outlined previously.[18] Li^+−fluorohectorite (F, exchange capacity = 150 mequiv/100 g, Corning Inc.), Li^+−saponite (S, exchange capacity = 100 mequiv/100 g, Southern Clay Products), and Na^+−montmorillonite (M, exchange capacity = 80 mequiv/100 g, Swy-1, University of Missouri Source Clay Repository) were used as received. Organic modifiers included dioctadecyldimethylammonium bromide (2C18, $2C_{18}H_{37}N^+2CH_3Br^-$, Kodak), octadecyltrimethylammonium bromide (Q18, $C_{18}H_{37}N^+(CH_3)_3Br^-$, Aldrich), and a series of primary alkylammonium chlorides ($C_nH_{2n+1}NH_3^+Cl^-$, where n = 6, 9−16, and 18). The primary alkylammonium cations were synthesized by acidifying a solution of the corresponding amine (Aldrich Chemical) with 1 M HCl. All OLS's were dried in a vacuum oven at 100−130 °C and stored in a vacuum desiccator with P_2O_5 until use. The characteristics of the different polymers used in this study are summarized in Table 1.

In general, hybrids were synthesized using the following procedure. Dry organosilicate (25 mg) and polymer powder (75 mg) were mechanically mixed and formed into a pellet using a hydraulic press at a pressure of 70 MPa. This insured the OLS was in the presence of excess polymer melt. Hybrid formation was accomplished by statically annealing the pellet in vacuum at temperatures greater than the glass transition temperature of the polymer and quenching in air to room temperature. Unless otherwise indicated, the samples were annealed to equilibrium, indicated by no further changes in the X-ray diffraction pattern.

3.2. Characterization. X-ray diffraction spectra were collected on a Scintag Inc. Θ−Θ diffractometer equipped with an intrinsic germanium detector system using either Cu Kα or Cr Kα radiation. After the raw diffraction data were corrected with the Lorenz-polarization powder factor and linear background subtraction, the location and width of the X-ray reflections were determined by profile fitting a Pearson VII function to the diffraction peak.[24] All X-ray diffraction spectra were collected from samples that were quenched in air from the anneal temperature.

4. Results

The outcome of an anneal was determined using X-ray diffraction measurements by monitoring the position,

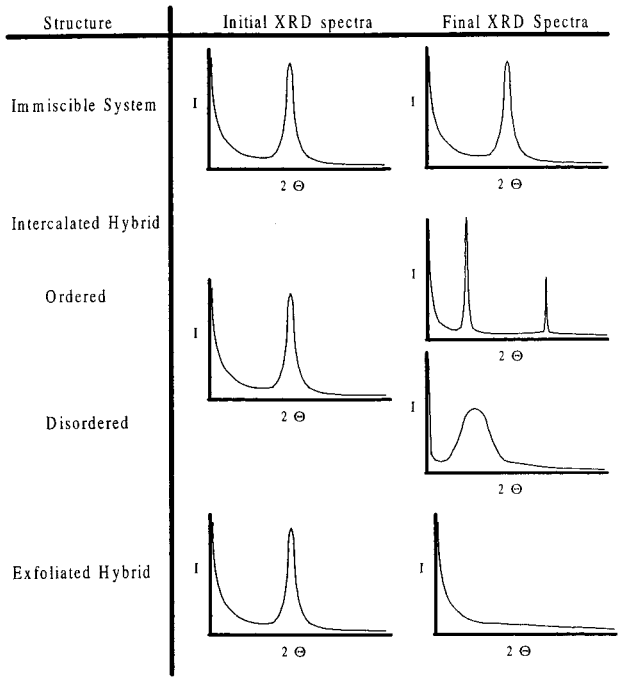

Figure 1. Schematic depicting the expected X-ray diffraction patterns for various types of hybrid structures.

full-width-at-half-maximum (fwhm), and intensity of the (001) basal reflection of the OLS. Figure 1 summarizes the corresponding X-ray spectra for various types of nanocomposites. For immiscible polymer/OLS mixtures, the structure of the silicate is not affected by the anneal, and thus, the characteristics of the OLS basal reflection do not change. On the other hand, the finite layer expansion associated with intercalated structures results in a new basal reflection that corresponds to the larger gallery height of the intercalated hybrid. In contrast, the extensive layer separation associated with exfoliated structures disrupts the coherent layer stacking and results in a featureless diffraction pattern. The influence of polymer intercalation on the order of the OLS layers may be monitored by changes in the fwhm and intensity of the basal reflections. An increase in the degree of coherent layer stacking (i.e. a more ordered system) results in a relative decrease in the fwhm of the basal reflections upon hybrid formation. On the other hand, a decrease in the degree of coherent layer stacking (i.e. a more disordered system) results in peak broadening and intensity loss.

4.1. Packing Density, Ammonium Head Group, and Surface Charge. Table 2 summarizes the results for reactions carried out at 170 °C between PS30 and various octadecylammonium-modified OLS's. The gallery height is calculated from the difference between the repeat distance, d_{001}, and the thickness of a silicate layer, 0.95 nm.[14−16] Annealing F18, FQ18, M2C18, and S2C18 with polystyrene yields intercalated hybrids. However, increasing the host area per octadecyl chain, as with M18 and S18, results in immiscible, unintercalated systems. Similarly, decreasing the host area per octadecyl chain, as with F2C18, also leads to an unintercalated system. At low interlayer packing densities of the organic modifier, the chains adopt a disordered monolayer arrangement. As the packing density increases, the chains adopt more extended conformations (and thus larger initial gallery heights), ultimately resulting in a solid-like paraffinic arrangement of the chains.[17,18] Therefore, an intermediate range of host area per aliphatic chain and thus an intermediate range of interlayer chain conformations are most favorable for polystyrene melt intercalation.

The difference between primary and quaternary ammonium head groups does not appear to be a predominant factor for polystyrene intercalation. Both primary (F18) and quaternary (FQ18) octadecyl modifiers result in intercalated hybrids. However, the different type of ammonium head group does influence the net gallery height increase and the final gallery height of the intercalated hybrid—the net gallery height change for FQ18 is about 0.29 nm more than that for F18. The additional gallery height increase may reflect the larger size of the quaternary ammonium head group and the more delocalized cationic charge compared to that of the primary ammonium head group.

In addition to the type of head group, the number of head groups per host area does not appear to be a determining factor. If the number of head groups was significant, the results in Table 2 should depend on the area per cation and not per chain. This is not the case. For example, M2C18 and M18 have the same number of head groups, but polystyrene intercalation occurs for M2C18 and not for M18. Furthermore, F18 has twice the number of ammonium groups as M2C18, but both OLS's lead to intercalated hybrids.

Finally, the results in Table 2 also indicate that the state of the polystyrene−OLS hybrid, whether intercalated or immiscible, is independent of the distribution of the anionic charge on the silicate surface. The negative charge of the silicate layers arises from isomorphous substitution in the crystal lattice. The location of the isomorphous substitution determines the distribution of excess negative charge on the layer surface and, therefore, the nature of guest interactions with the silicate surface.[14−16] The increased localization of surface charge for tetrahedrally-substituted saponite does not appear to critically affect hybrid formation when compared to the more disperse surface charge of octahedrally-substituted montmorillonite.

4.2. Chain Length and Anneal Temperature. Figure 2 shows the final gallery height and full-width-at-half-maximum (fwhm) of a series of PS30−F*n* samples annealed at 120, 140, and 160 °C; *n* is the number of carbon atoms of the aliphatic chain in the organosilicate. The gallery heights of pure F*n*'s annealed at 160 °C are included for comparison. For $n \leq 12$, the gallery height of the unintercalated F*n* is constant and the aliphatic chains are arranged in a pseudo-bilayer, with the highest segment density at $n = 12$. For $n > 12$, the layer spacing increases and the chains adopt disordered pseudo-trilayer to liquid crystal-like arrangements.[17,18]

In general, the intercalation behavior of the F*n* series is independent of anneal temperature between 120 and 160 °C but critically depends on the length of the chain, *n*. For pseudo-bilayer chain arrangements ($n < 12$), no polymer intercalation occurs. With the exception of a small increase in the fwhm of the peaks at 160 °C, the characteristics of the basal reflection, and thus the structure of the F*n*'s, do not change. For $n > 12$, intercalated hybrids are formed, as evidenced by the gallery height increases. The full-width-at-half-maximum of the basal reflections of the intercalated structure is comparable to that of the original unintercalated silicate, indicating that polymer intercalation does not disrupt the stacking order of the silicate layers. For a full pseudo-bilayer ($n = 12$) though, intercalated basal reflections are observed with intensities less than and breadths greater than those observed for the annealed

Table 2. Summary of Polystyrene (PS30) Melt Intercalation of Octadecylammonium-Modified OLS's

OLS	area/cation, nm^2	area/chain,[a] nm^2	initial gallery height,[b] nm	final gallery height,[b] nm	het change, nm	model[c]
M18	0.72	0.72	0.75	0.75	0	
S18	0.58	0.58	0.83	0.83	0	
F18	0.39	0.39	1.33	2.16	0.83	intercalated
FQ18	0.39	0.39	1.57	2.69	1.12	intercalated
M2C18	0.72	0.36	1.43	2.25	0.82	intercalated
S2C18	0.58	0.29	1.50	2.35	0.85	intercalated
F2C18	0.39	0.20	2.85	2.85	0	immiscible

[a] Area per unit cell of aluminosilicate layer is 0.465 nm^2.[14–16] [b] Gallery height = d_{001} − 0.95 nm. [c] Predicted hybrid states using parameters in Table 4.

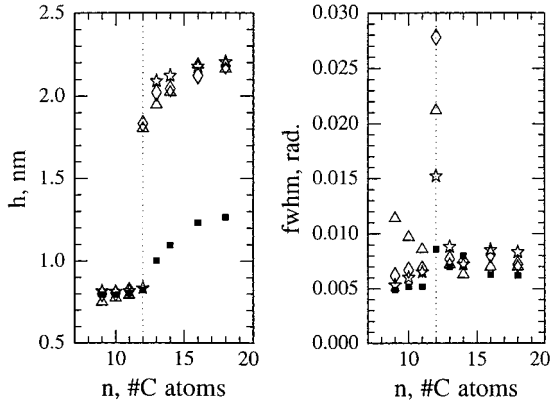

Figure 2. Final gallery height, h, and full-width-at-half-maximum, fwhm, of a series of PS30−F*n* samples annealed at 120 °C (☆), 140 °C (◇), and 160 °C (△) and pure F*n* samples annealed at 160 °C (■).

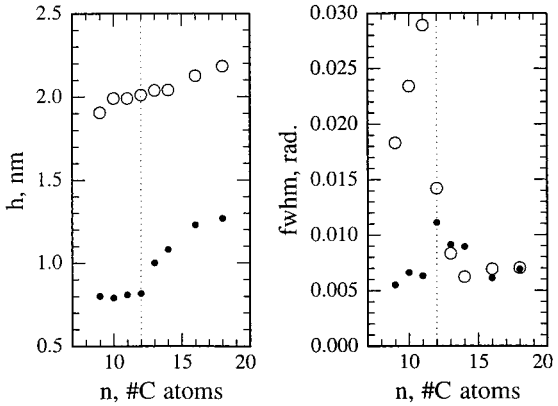

Figure 4. Final gallery height, *h*, and full-width-at-half-maximum, fwhm, of a series of PS30−F*n* samples annealed at 180 °C (○) and pure F*n* samples annealed at 180 °C (●).

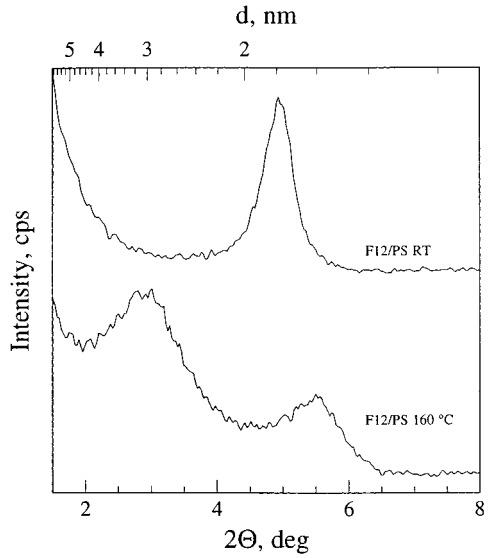

Figure 3. X-ray diffraction patterns of a PS30−F12 sample before and after annealing at 160 °C in vacuum.

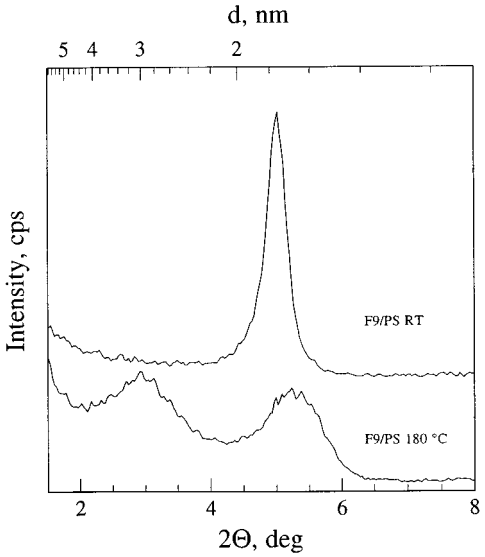

Figure 5. X-ray diffraction patterns of a PS30−F9 sample before and after annealing at 180 °C in vacuum.

F12 host. Figure 3 compares a PS30−F12 mixture before annealing and after annealing at 160 °C. (The X-ray pattern of F12 for these conditions is independent of anneal time and temperature.) In contrast to the case for $n > 12$ and previous polystyrene−OLS hybrids, polymer intercalation of F12 disrupts the silicate layers, producing a more disordered intercalated hybrid.

Increasing the anneal temperature to 180 °C alters the intercalation behavior of the F*n* series for $n \leq 12$. Figure 4 summarizes the results for F*n* and PS30−F*n* samples annealed at 180 °C. F*n*'s annealed in the absence of polymer at these conditions exhibit similar scattering behavior to that observed at lower anneal temperatures (Figure 2), indicating the F*n*'s are thermally stable up to 180 °C. For PS30−F*n* admixtures with $n > 12$, intercalated hybrids form with gallery heights comparable to those formed at lower anneal temperatures. For all the bilayer chain arrangements ($n \leq 12$) however, the X-ray spectra contain broadened basal reflections corresponding to a disordered intercalated structure. For example, Figure 5 compares a PS30−F9 mixture before annealing and after annealing at 180 °C. The characteristics are similar to those displayed by PS30−F12 at the lower anneal temperatures.

These results indicate that a bilayer chain arrangement and higher anneal temperatures favor the formation of hybrids in which the stacking of the silicate layers is disrupted. Because the samples are statically annealed, transport of the silicate layers over macro-

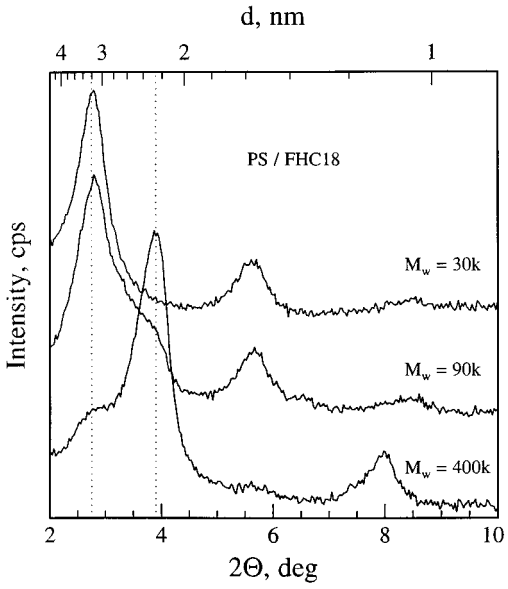

Figure 6. X-ray diffraction patterns of PS30−F18, PS90−F18, and PS400−F18 annealed 6 h in vacuum at 160 °C.

scopic distances to produce an exfoliated state would take a prohibitively long time. Therefore, this behavior may be indicative of a kinetically-limited exfoliated structure.

4.3. Polymer Molecular Weight. Figure 6 shows the X-ray diffraction patterns of PS30−F18, PS90−F18, and PS400−F18 after a 6 h anneal in vacuum at 160 °C. All three samples were prepared in an identical fashion using the same host particle size. The PS30−F18 pattern contains diffraction peaks characteristic of only the intercalated hybrid. The PS90−F18 and PS400−F18 patterns though contain peaks characteristic of both intercalated (2θ = 4.15 and 8.03°) and unintercalated OLS (2θ = 2.82 and 5.66°). Fully intercalated hybrids for PS90 and PS400 are formed after annealing at 160 °C for 24 and greater than 48 h, respectively. The fwhm of the intercalated basal reflection is approximately the same for all molecular weights. Thus for statistically annealed PS samples, the final hybrid structure is independent of the molecular weight of the polymer. In this case, the molecular weight only appears to affect the kinetics of polymer intercalation. These observations agree with those of previous studies of the kinetics of polymer melt intercalation where the final hybrid structure was found to be independent of the polymer molecular weight as well as the particle size of constituents, the degree of powder mixing, and the processing (static or use of shear blending).[4] However, the model[1] indicates that there should be a slight molecular weight dependence for melt intercalation which arises from the entropy change of the polymer. Additional experimental work examining the intercalation behavior of a broader range of polymer molecular weights coupled with dynamic blending of constituents to enhance equilibrium mixing is required to further explore this issue.

4.4. Intermolecular Interactions. Table 3 summarizes the results of melt intercalation of a series of styrene-derivative polymers with M2C18 and F2C18. All the polymers are immiscible with F2C18. On the other hand, all polymers but poly(vinylcyclohexane), PVCH, form intercalated hybrids with M2C18, indicating that the structure of the pendant group on the polymer greatly affects hybrid formation.

Table 3. Summary of Melt Intercalation of M2C18 and F2C18 with Styrene-Derivative Polymers

Polymer	Net Gallery Height Increase, nm M2C18	F2C18
PVCH	0.00	0.00
PS	0.82	0.00
PS3Br	0.96 [a]	0.00
PVP	1.00 [b]	0.00

[a] Intensity decreases observed associated with increased absorption of Br. [b] Peak broadening and intensity decrease of d_{001}.

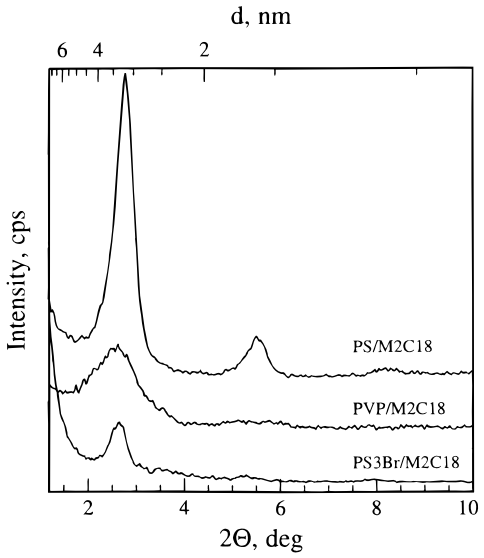

Figure 7. X-ray diffraction patterns of PS−M2C18, PVP−M2C18, and PS3Br−M2C18 hybrids with the same volume percent M2C18 (20%).

Figure 7 compares the X-ray diffraction patterns of poly(vinylpyridine) (PVP), poly(3-bromostyrene) (PS3Br), and PS30 hybrids containing the same volume percent of M2C18. As discussed before, polystyrene produces a well-ordered intercalated hybrid. Bromination of the phenyl ring in the meta position (PS3Br) produces an intercalated hybrid similar to polystyrene but with a slightly larger gallery height. The intensity of the intercalated basal reflection, though, is reduced approximately 50% with respect to that of the unintercalated PS3Br−F18 mixture, but the fwhm of the intercalated reflection remains unchanged. The large decrease in the intensity of the basal reflection of PS3Br−M2C18 is partially due to the large absorption coefficient of the bromine atom that, when intercalated, decreases the overall scattering factor of the silicate/polymer layer structure. Substituting the ortho carbon with nitrogen (PVP), produces a disordered intercalated structure that is similar to that observed for PS30−F12. The basal reflections of the PVP−M2C18 hybrid are substantially broader (0.019 rad) than those observed

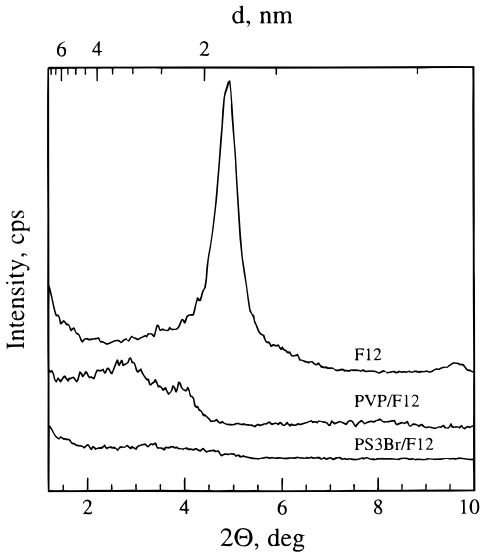

Figure 8. X-ray diffraction patterns of PS3Br−F12, PVP−F12, and pure F12.

for PS30−M2C18 (0.007 rad), indicating that the coherent length of the silicate layers in the PVP hybrid is less than that of those in the PS30 hybrid.

Melt intercalation of M2C18 with these polymers emphasizes the importance of polar interactions during hybrid formation. Since the backbone of the styrene-derivative polymers is comprised of a saturated hydrocarbon, polar interactions arise from the relative acid/base character and degree of polarizability of the pendant ring. From small molecule analogs, the asymmetry of the electron density distribution of the pendant ring and thus the polarizability increases in the order PVCH << PS < PS3Br, PVP.[25] As we move along this series, the hybrid structure changes. Since PVCH is essentially nonpolar,[26] only van der Waals interactions are present and an immiscible system is obtained. In contrast, because of the electron-donating nature of the phenyl group in PS, polar interactions are now possible, leading to an intercalated hybrid. Increasing the electron density and polarity of the pendant group, as in PVP, results in more disordered hybrid structures.

It is interesting to note that the kinetics of hybrid formation for PVP and PS3Br, even when taking into account the differences in molecular weight, are noticeably slower than those for PS (greater than 24 h versus less than 4 h). In addition to the presence or absence of shear and the molecular weight of the polymer, the kinetics appear to depend on the degree of interaction between the polymer and OLS, possibly manifesting in an increase of the effective monomer friction coefficient within the interlayer with increased polymer−OLS interactions.

In the previous section, we noted that bilayer structures of the organic modifiers favor the formation of disordered hybrids with polystyrene. Combining these OLS's with PVP and PS3Br may produce hybrids which are even more disordered or even exfoliated. Figure 8 shows the X-ray diffraction spectra for PVP-F12 and PS3Br-F12 containing the same volume percent of silicate (20%). Also included in the figure is the X-ray pattern of pure F12 annealed at the same conditions. Compared with the case of PS30−F12 in Figure 3, the basal reflections of PVP−F12 and PS3Br−F12 around $2\theta = 2.8°$ are much weaker and substantially broader, indicating a very disordered hybrid. PVP−F12 also displays a second, narrower reflection at 2Q = 3.8 that may correspond to an intermediate intercalated structure. The intensity decrease of PS3Br−F12 is greater than that attributed to the increased absorption of the bromine atom seen for PS3Br−M2C18. Since the kinetics are slower for these polymers, the structures observed may be kinetically limited because of the static processing.

5. Discussion

Two major qualitative trends may be drawn for the systematic experimental study just outlined. First, there is an optimum interlayer structure favoring hybrid formation that is intermediate between a disordered monolayer and a solid-like paraffinic arrangement of aliphatic chains.[18] For the polystyrene-derivative systems studied, the optimum interlayer structure is near a full pseudo-bilayer. Second, polar-type interactions (i.e. other than van der Waals) are critical for formation of intercalated and especially exfoliated hybrids via polymer melt intercalation.

These results are counterintuitive. To minimize polymer confinement and facilitate layer separation, polymer intercalation would be expected to be most favorable for OLS's that are modified such that the initial gallery height is maximized. This occurs for solid-like paraffinic arrangement of chains when the host area available per chain approaches the van der Waals cross-sectional area of a chain. Additionally, since the silicate interlayer is modified by aliphatic chains, apolar or van der Waals-type interactions between the OLS and the polymer should dominate and hybrid formation would be most favorable for "aliphatic-like" polymers, such as polyethylene, saturated polyolefins, PVCH, etc. These conclusions are not supported by experimental results and in fact describe situations in which polymer intercalation is unfavorable.

Insight into the factors controlling polymer melt intercalation may be obtained by comparing the experimental results to the theoretical predictions of the mean-field model.[1] Using this model, the following sections examine how various aspects, including the nature of the polymer and OLS, affect the thermodynamics of polymer intercalation. After identifying the important system parameters, we discuss a framework which allows the construction of product maps and outline general guidelines that govern hybrid formation.

5.1. Entropy. The entropy change per interlayer volume, Δs_V, is comprised of two competing factors (eq 2)—an entropy decrease per interlayer volume associated with confinement of the polymer upon intercalation, $\Delta s_V^{polymer}$, and an entropy increase per interlayer volume associated with conformational freedom of the aliphatic chains upon layer separation, Δs_V^{chain}.

To examine the influence on hybrid formation of the length of the aliphatic chain and the area per aliphatic chain, it is useful to express the initial gallery height, h_0, in terms of the number of aliphatic chains per interlayer area, σ, the number of segments in an aliphatic chain, m_2, and the volume of an aliphatic segment, v_2/N_A.

$$h_0 = \sigma m_2 v_2 / N_A \tag{7}$$

As discussed in the previous paper, we define a chain segment as a C_2H_4 unit.[1] The number of segments per chain is $(n + 1)/2$, where the additional unit represents the head group of the alkyl ammonium cation.

Figure 9 demonstrates the effect of increasing the initial gallery height, by increasing the number of

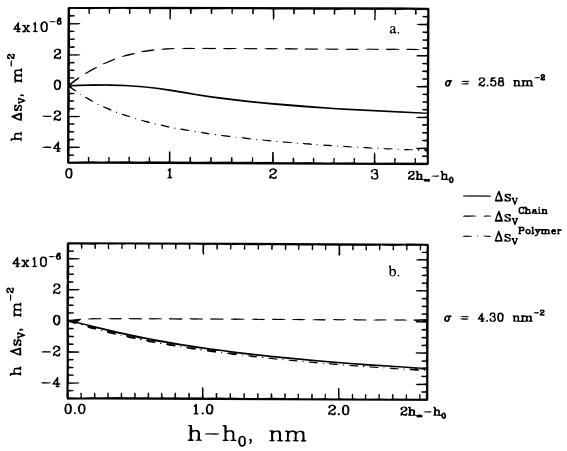

Figure 9. Effect of increasing the number of aliphatic chains per area, σ (a, $\sigma = 2.58$ nm^{-2}; b, $\sigma = 4.30$ nm^{-2}), on the entropy per interlayer area of polymer intercalation as the net change in gallery height, $h - h_0$, increases. The curves are calculated using the parameters in Table 4 and eq 2. h_o is the initial gallery height of the interlayer, and h_∞ is the fully extended length of the aliphatic chain. Note that the scales of the abscissas are different, since h_0 is related to σ.

Table 4. Parameters for Polystyrene and F*n* Used in the Model Calculations[a]

polystyrene		F*n*	
parameter	value	parameter	value
a_1[b]	0.38 nm	a_2	0.25 nm
v_1[c]	99 cm^3	v_2[d]	32 cm^3
$u/\sqrt{m_1}$	0.8	σ[e]	2.58 nm^{-2}
γ_p^{LW} [f]	42.0 mJ m^{-2}	γ_s^{LW} [g]	66 mJ m^{-2}
γ_p^{+} [f]	0.0 mJ m^{-2}	γ_s^{+} [f]	0.7 mJ m^{-2}
γ_p^{-} [f]	1.1 mJ m^{-2}	γ_s^{-} [f]	36.0 mJ m^{-2}
		γ_a^{LW} [f]	26.0−28.5 mJ m^{-2}

[a] Interaction parameters, ϵ_{ap} and $\epsilon_{sp,sa}$, are approximated from values of interfacial energies using eq 4−6.[27] [b] $a_1 = a_p(v_2/v_1)^{1/2}$, where a_p is the statistical segment length of polystyrene (0.67 nm).[1,20] [c] Reference 29. [d] Ratio of formula weight per mole of aliphatic segments and average interlayer density (0.9 g/cm^3).[1,19] [e] (Number of chains/Si_8O_{20} unit)/(0.465 nm^2/Si_8O_{20} unit). [f] References 21−23. [g] Estimated from the Hamaker constant.[30]

aliphatic chains per area ($\sigma = 2.58$ nm^{-2} to $\sigma = 4.30$ nm^{-2}), on the entropic components $h\Delta s_V^{polymer}$, $h\Delta s_V^{chain}$, and $h\Delta s_V$. Note that the entropy density is an extensive quantity because the volume of the system varies linearly with interlayer spacing. In contrast, the product of the entropy density in the interlayer and the gallery height is an intensive quantity and independent of system size. Table 4 summarizes the values for the theoretical parameters used in the calculation.

Figure 9a ($\sigma = 2.58$ nm^{-2}) depicts the entropy change per area for $n = 18$. For small increases in the gallery height, the entropy gain associated with the tethered aliphatic chains approximately nullifies the entropy loss due to polymer confinement. Here, small favorable internal energy changes will lead to a free energy decrease and thus hybrid formation. As the gallery height increases, however, the magnitude of the entropy loss due to polymer confinement increases and the total entropy change decreases. Hybrid formation becomes less likely.

As the number of the aliphatic chains per area increases (Figure 9b), the initial gallery height increases, resulting in a smaller entropic penalty for polymer confinement. However, the increased number of chain segments per area leads to a decrease in the entropy gain of the aliphatic chains. The subsequently tighter-packed chains do not gain as much conformational freedom when the layer separation increases.[1] Therefore, the total entropy change becomes increasingly unfavorable, and immiscible systems are more likely. OLS's with a higher chain-packing density generally exhibit a paraffin-type arrangement of chains in the interlayer, as in F2C18. The inability of the aliphatic chains to gain conformational freedom probably contributes to the inability to intercalate F2C18 (Table 3).

In general, the model indicates that the entropy associated with the aliphatic chains only increases until the tethered chains are fully extended. Further layer separation depends on the establishment of very favorable interactions to overcome the continually increasing penalty of polymer confinement.[1] For polymers with weak associative interactions, such as polystyrene, the penalty of polymer confinement for layer separations greater than the length of the fully extend aliphatic chain will not be compensated. Thus, intercalated hybrids with gallery heights near the length of the fully extended chain would be expected. This is the case for intercalated polystyrene hybrids in Table 2 and for PS-F*n*'s with $n > 12$ in Figures 2 and 4.[31]

When the gallery area available is greater than the lateral cross-sectional area of the chains, a pseudobilayer is formed. These structures are outside the boundaries of the mean-field model because their interlayer does not initially have 'fully-occupied' lattices.[1,19] For the F*n* series, interlayers not 'fully-occupied' correspond to $n < 12$. Qualitatively though, as the area available per chain increases above the lateral cross-sectional area of the chain, the number of chain segments that gain conformational freedom as the layers separate decreases. Subsequently, the magnitude of Δs_V^{chain} decreases. Additionally, the smaller initial gallery height results in a larger penalty for polymer confinement. Hence, as with paraffin-type structures, hybrid formation should also be entropically less favorable for short chain lengths or interlayers with low chain-packing density. The intercalation behavior of PS-F*n*'s with $n < 12$ as temperature increases is thus related to energetic changes in the system and not entropic changes. Combining these qualitative arguments with the results from the model indicates that, entropically, hybrid formation is most favorable for OLS's with intermediate gallery heights and packing densities, in agreement with experimental results for the octadecylammonium-modified OLS's in Table 2 and the F*n* series in Figures 2 and 4.

5.2. Internal Energy. From the thermodynamic model, the energy change for hybrid formation (eq 3) depends on the sign and magnitude of the interaction parameters (ϵ_{jk}) and on the initial interlayer structure of the OLS (Q, h_0, and r_2). In general, for small, favorable internal energy changes, intercalated states are expected. As the change in internal energy becomes more negative, the tendency to form exfoliated hybrids increases.[1] We will first consider the effect of the interaction parameters on the internal energy change of the system.

5.2.1. Interaction Parameters. The interaction parameters, ϵ_{jk}, express the relative energy change associated with the establishment of contacts between the polymer, aliphatic chains, and the interlayer surface. The interaction energy within the interlayer volume corresponds to the energy of polymer−aliphatic contacts, ϵ_{ap}, whereas the interaction energy at the

interlayer surface corresponds to the replacement of aliphatic−surface contacts by polymer−surface contacts, $\epsilon_{sp,sa}$.[32]

Since the aliphatic chains are apolar ($\gamma_a^+ = \gamma_a^- = 0$), dispersive, van der Waals-type interactions will determine the sign and magnitude of ϵ_{ap}. Equation 5 indicates that these interactions at best will be equal to zero for apolar polymers with surface energies similar to those of the aliphatic chains ($\gamma_a^{LW} \sim \gamma_p^{LW}$). If these dispersive interactions drove polymer intercalation, hybrid formation would be energetically most favorable for polyalkanes and saturated polyolefins. Experimentally though, these polymers lead to immiscible hybrids (PVCH (Table 3), polyethylene[19]) in static experiments.[33]

Thus, the favorable internal energy change driving polymer intercalation arises from interactions at the interlayer surface, $\epsilon_{sp,sa}$ and $\Delta\gamma_s$. If the polymer interacts more favorably with the surface than the aliphatic chain, $\epsilon_{sp,sa} < 0$. From eq 4 and 6, favorable interactions arise when $\gamma_{jk}^{AB} < 0$ and $|\gamma_{jk}^{AB}| > \gamma_{jk}^{LW}$. Two conditions exist for a negative γ_{jk}^{AB}: $\gamma_j^+ > \gamma_k^+$ and $\gamma_j^- < \gamma_k^-$, or $\gamma_j^+ < \gamma_k^+$ and $\gamma_j^- > \gamma_k^-$.[21−23] Physically, these conditions imply that each interacting species possesses either the strongest electron donating or electron accepting moiety but not both.

For the styrene-derivative polymers examined, these interactions most likely occur between the interlayer surface and the pendant groups of the polymers (Table 3). For polystyrene, the resonance structure of the phenyl ring exhibits a slight Lewis-base character.[21] For PVP and PS3Br, the electronegative additions in the pendant ring redistribute the ring's electron density. Possible Lewis-acid sites on the silicate include the cationic head group of the organic modifier or the Si^{4+} atoms in the tetrahedral sites of the silicate layer, while possible Lewis-base sites include the surface oxygens of the layer.[14−16,35,36] Since to maximize compatibility monopolar (i.e. either Lewis acids or bases) components are required, as the basic character of the polymer increases, organosilicates with strong electron accepting and weak electron donating properties are needed.

5.2.2. Initial Interlayer Structure. In addition to the sign and magnitude of the interaction parameters, the internal energy change depends on the relative contribution of these interactions. The relative contribution is determined by the fraction of the various interaction sites within the gallery. This depends on the initial interlayer structure of the OLS. From the model, the relative number of the various interaction sites is expressed by the critical interlayer structure parameter, ξ_C, which is the ratio of the geometrical prefactors of the interaction parameters in eq 3.[1] For large initial gallery heights (large ξ_C), the interactions within the interlayer between polymer and aliphatic segments, ϵ_{ap}, contribute the most to the internal energy change. For OLS's with smaller initial gallery heights (smaller ξ_C), the interactions at the interlayer surface, $\epsilon_{sp,sa}$, contribute increasingly more to the energy change.

Recall that, for OLS's with aliphatic chains, ϵ_{ap} is greater than zero, and thus $\epsilon_{sp,sa}$ must be less than zero for an energetic decrease upon hybrid formation. Note that the polar moieties of the polymer, which are necessary for the establishment of more favorable surface interactions, will be deleterious for interactions with the apolar aliphatic chains within the interlayer volume (eq 6). Thus, the optimal OLS interlayer structure will minimize the number of potential interactions within the interlayer, while maximizing the number of potential replacement sites on the interlayer surface.

A comment is warranted at this time concerning melt intercalation of layered silicates modified with organic chains possessing polar moieties such as phenyl, alcoholic, ester, etc. Proper choice of these moieties will result in more favorable interactions between the polymer and organic modifier, potentially leading to $\epsilon_{ap} < 0$ and very favorable conditions for melt intercalation. However, introduction of these moieties may also be deleterious. If these polar groups have very favorable interactions with the silicate surface, replacement of surface contacts will be difficult and the effective number of contacts between the polar groups and the polymer in the interlayer will decrease. Similarly, the entropic gain associated with the increase in conformational freedom of the organic chains will decrease. These effects will impede hybrid formation. A careful weighing of all these considerations is necessary to select the optimal interlayer functionalization.

Qualifying the influence of the initial interlayer structure and the various interlayer interactions on hybrid formation may lead to a criterion to select potentially successful polymer−OLS systems. One potential approach to determining the equilibrium state for a polymer/OLS system is to calculate the free energy change per area using eq 1−6. Using values in Table 4, we determined the equilibrium states for various Fn−PS systems ($12 \le n \le 18$) from the minimum of the free energy change per area as a function of gallery height.[1] In all cases intercalated hybrids are predicted in agreement with the experiment. The final gallery heights predicted from the model for different chain lengths also exhibit the same trend (decreasing intercalated gallery height with decreasing n) found experimentally (Figures 2 and 4). Within the framework of the model, the effect of varying chain length parallels that for varying the area per chain, since both contribute linearly to h_0 (eq 7). Therefore, assuming the interaction parameters are the same for the different OLS's, the hybrid state predicted for OLS's with various areas per chain (Table 2) also agrees with the equilibrium states observed. However, the magnitude of the net gallery height increase calculated from the model differs from experimental values by up to 35%. This is not surprising though given the simplicity of the theoretical formulation and the uncertainty of the values of the parameters used.

5.3. Product Maps. An alternative approach to using the free energy curves to determine the favored equilibrium state is to derive a 'product map' (similar to a phase diagram) for a given set of parameters. The product maps display the dependence of the sign of the internal energy change on two system parameters. As outlined in the previous paper,[1] the total entropy change, to a first approximation, is near zero for the initial stages of polymer intercalation. For these cases, the sign of the internal energy change will determine the sign of the free energy change of the system and, thus, the outcome of intercalation. Within the bounds of the model, the total energy is near zero when $|\epsilon_{sp,sa}/\epsilon_{ap}| = \xi_C$.[1] Determining ξ_C from the initial interlayer structure and using eqs 4−6 to express $\epsilon_{sp,sa}$ and ϵ_{ap}, the resulting equality gives the dependence of the point of zero energy change on the various apolar and polar interaction parameters of the constituents. From the perspective of establishing a methodology for selecting

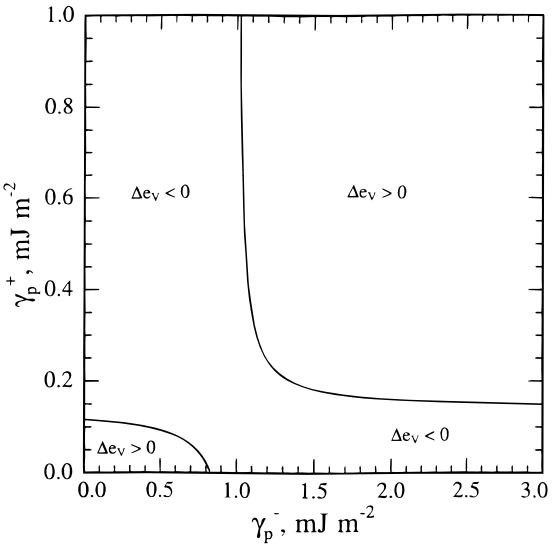

Figure 10. Product map showing the dependence of the internal energy change per interlayer volume on the Lewis acid, γ_p^+, and Lewis base, γ_p^-, parameters of a polymer (γ_p^{LW} = 42 mJ m^{-2}) with an 'octadecyl'-modified silicate. Curves are determined using the surface tension parameters in Table 4 and $\xi_C = 5.0$.

successful polymer/OLS combinations, the product maps are more instructive than the free energy curves because the effects of various parameters on the equilibrium state are more readily discernible.

For example, using parameters for the OLS outlined in Table 4, Figure 10 shows the relationship between the Lewis-acid, γ_p^+, and Lewis-base, γ_p^-, components of the polymer interfacial energy for intercalation of a polymer ($\gamma_p^{LW} = 42$ mJ m^{-2}) into an 'octadecyl'-modified silicate. Similar maps may be constructed displaying the relationships between other interaction parameters, such as intercalation of a given polymer into modified silicates with different γ_s^+ and γ_s^-. In the central region of Figure 10, the internal energy change, and thus the free energy change of the system, is less than zero, and hybrid formation is favorable. For polymers with parameters outside this region, the net energy change is greater than zero and hybrid formation is unfavorable. In principle, the potential product of polymer melt processing may be determined *a priori* from values of the surface interaction energies. Because of the limited availability of measured values of γ_j^+, γ_j^-, and γ_j^{LW}, a comprehensive comparison with experiment is difficult. However, for the values available, the product maps agree well with the experiments.[19] Currently, we are exploring ways to better quantify the various interaction parameters.

6. Conclusions

Experimental results indicate that the outcome of polymer intercalation depends critically on silicate functionalization and constituent interactions. We observed that (a) an optimal interlayer structure of the OLS, with respect to the number per area and size of the alkylammonium chains, is most favorable for hybrid formation and (b) polymer intercalation depends on the existence of polar interactions between the OLS and the polymer.

In general, the conclusions of the mean-field model described previously[1] agree with the experimental results. The entropy loss associated with confinement of a polymer melt is not prohibitive to hybrid formation because an entropy gain associated with layer separation balances the entropy loss of polymer intercalation, resulting in a net entropy change near zero. Thus, from the theoretical model, the outcome of hybrid formation via polymer melt intercalation depends on energetic factors which may be determined from the surface energies of the polymer and OLS.

From these observations and the construction of product maps, general guidelines may be established for selecting potentially compatible polymer−OLS systems. Initially, the interlayer structure of the OLS should be optimized to maximize the configurational freedom of the functionalizing chains upon layer separation and to maximize potential interaction sites at the interlayer surface. For these systems, the optimal structure appears to exhibit a chain arrangement slightly greater than a pseudo-bilayer. Polar polymers containing groups capable of associative-type interactions, such as Lewis-acid/base interactions or hydrogen-bonding, lead to intercalation. The greater the polarizability or hydrophilicity of the polymer, the shorter the functionalizing groups in the OLS should be to minimize unfavorable interactions between the aliphatic chains and the polymer.

Acknowledgment. This work was supported by NSF (DMR-9424446) and by generous gifts from DuPont, Exxon, Hercules, Monsanto, Nanocor, Southern Clay Products, and Xerox. R.A.V. gratefully acknowledges the partial support of a NDSEG Fellowship. We would like to thank L. Vega and R. Krishnamoorti for fruitful discussions. This study benefited from the use of Material Science Central Facilities at Cornell.

References and Notes

(1) Vaia, R. A.; Giannelis, E. P. *Macromolecules* **1997**, *30*, 7990.
(2) Vaia, R. A.; Ishii, H.; Giannelis, E. G. *Chem. Mater.* **1993**, *5*, 1694.
(3) Vaia, R. A.; Vasudevan, S.; Krawiec, W.; Scanlon, L. G.; Giannelis, E. P. *Adv. Mater.* **1995**, *7*, 154.
(4) Vaia, R. A.; Jandt, K. D.; Kramer, E. J.; Giannelis, E. P. *Macromolecules* **1995**, *28*, 8080.
(5) Vaia, R. A.; Jandt, K. D.; Kramer, E. J.; Giannelis, E. P. *Chem. Mater.*, in press.
(6) Burnside, S. D.; Giannelis, E. P. *Chem. Mater.* **1995**, *7*, 1597.
(7) Usuki, A.; et al. *J. Mater. Res.* **1993**, *8*, 1179.
(8) Yano, K.; Usuki, A.; Kurauchi, T.; Kamigaito, O. *J. Polym. Sci., Part A: Polym. Chem.* **1993**, *31*, 2493.
(9) Messersmith, P. B.; Giannelis, E. P. *Chem. Mater.* **1994**, *6*, 1719.
(10) Messersmith, P. B.; Giannelis, E. P. *J. Polym. Sci., Part A: Polym. Chem.* **1995**, *33*, 1047.
(11) Aranda, P.; Ruiz-Hitzky, E. *Chem. Mater.* **1992**, *4*, 1395.
(12) Vaia, R. A.; Sauer, B.; Giannelis, E. P. Submitted to *J. Polym. Sci., Part B: Polym. Phys.* **1997**, *35*, 59.
(13) Wong, S.; Vasudevan, S.; Vaia, R. A.; Giannelis, E. P.; Zax, D. *J. Am. Chem. Soc.* **1995**, *117*, 7568.
(14) Pinnavaia, T. J. *Science* **1983**, *220*, 365.
(15) Brindley, S. W., Brown, G., Eds. *Crystal Structure of Clay Minerals and their X-ray Diffraction*; Mineralogical Society: London, 1980.
(16) Güven, N. In *Hydrous Phyllosilicates*; Bailey, S. W., Ed.; Reviews in Mineralogy Vol. 19; Mineralogical Society of America: Washington, DC, 1988; pp 497−560.
(17) For a detailed discussion of the interlayer structure of alkyl-modified OLS's, see ref 18 and references contained therein.
(18) Vaia, R. A.; Teukolsky, R. K.; Giannelis, E. P. *Chem. Mater.* **1994**, *6*, 1017.
(19) Vaia, R. A. Doctoral Thesis, Cornell University, 1995.
(20) Brandrup, J., Immergut, E. H., Eds. *Polymer Handbook*; John Wiley and Sons: New York, 1989.
(21) van Oss, C. J. *Interfacial Forces in Aqueous Media*; Marcel Dekker: New York, 1994.
(22) Norris, J.; Giese, R. F.; van Oss, C. J.; Costanzo, D. M. *Clays Clay Miner.* **1992**, *40*, 327.

(23) van Oss, C. J.; Chaudhury, M. K.; Good, R. J. *Sep. Sci. Technol.* **1989**, *24*, 15.
(24) Brown, A.; Linde, S. *Adv. X-ray Anal.* **1986**, *30*, 343.
(25) The asymmetric electron density of the ring moieties was approximated from ^{1}H NMR spectra of cyclohexane, toluene, pyridine, and 3-bromotoluene by comparing the relative shielding and deshielding of the ring protons.
(26) In contrast to the planar conformation of the rings with resonance structures, cyclohexane posses a boat conformation, and thus it might interact differently with the OLS. For a first approximation, we ignore these geometric effects.
(27) Experimental results reported by van Opstal et al.[28] for mixtures of polystyrene and short *n*-alkanes indicate that the upper critical miscibility temperature (USCT), and therefore the Θ condition, of these mixtures are near temperatures used for melt intercalation of polystyrene. This agrees with $\epsilon_{ap} \sim 0$ determined from the surface tensions, lending validity to our methodology of calculating values for the interaction parameters.
(28) van Opstal, L.; Konigsveld, R.; Kleintjens, L. A. *Macromolecules* **1991**, *24*, 161.
(29) Barton, A. F. M. *Handbook of Solubility Parameters and Other Cohesion Parameters*; CRC Press: Boca Raton, FL, 1983.
(30) Israelachvili, J. *Intermolecular and Surface Forces*; Academic Press: New York, 1992.
(31) The length of a fully-extended alkylammonium chain may be approximated as $(n' - 1)0.127 + A + B$ nm where n' is the number of carbon atoms and A and B are the size of an ammonium and a methyl group.[14−16]
(32) It may be argued that the polymer−OLS interlayer interactions are associated with dipole-induced interactions resulting from electrostatic fields arising from the anionically-charged silicate surface and the cationic organic modifiers. Assuming the cation head groups reside at the silicate surface,[19] the interlayer $\vec{E}$ field may be shown to be approximately zero using Gausses law. This is a reasonable assumption, since the cationic head group would prefer to reside close to the anionically-charged surface.
(33) Values for γ_p^{LW} are not available for some of the polymers used in the study. However, the dispersive interactions between the polymer and the aliphatic chains may be estimated by examining the difference in the dispersive cohesion energy densities, δ_d, of polymers and alkanes. From the literature, $\delta_d^{PVCH} = 15$,[34] $\delta_d^{PS} = 19.7$,[29] and $\delta_d^{alkane} = 16.6-16.8$ MPa$^{1/2}$.[29] The most favorable apolar interaction occurs when the difference in d_d's is zero. If dispersive interactions within the interlayer drove polymer intercalation, PVCH would be more favorable than PS. Experimentally, this is not the case (Table 3). Furthermore, polyethylene ($\delta_d^{PE} = 17.6$ MPa$^{1/2}$ [29]) would be even more favorable than both PS and PVCH. However, melt intercalation attempts between linear polyethylene and OLS's have been unsuccessful.[19]
(34) Gehlsen, M. D.; Bates, F. S. *Macromolecules* **1994**, *27*, 3611.
(35) Bleam, W. F.; Hoffman, R. *Inorg. Chem.* **1988**, *27*, 3180.
(36) Bleam, W. F.; Hoffman, R. *Phys. Chem. Miner.* **1988**, *15*, 398.

MA9603488